Check for updates

A Smoothing Aggregation Cascadic Multilevel Method for Image Deblurring

Pietro Maurino(✉) and Marco Donatelli

Department of Science and High Technology (DiSAT), Università degli Studi dell'Insubria, Como 22100, Italy
{pmaurino,marco.donatelli}@uninsubria.it

Abstract. We propose an Aggregation Cascadic Multiresolution method for image deblurring problems. Multigrid and multiresolution methods have already been studied in this context; see [4,6,7,12,13]. Here, we focus on a two-level cascadic multiresolution method with a specific choice of grid transfer operators.

The main novelty of our approach lies in the construction of both the prolongation and restriction operators, which are derived from a segmentation of the observed image. The restriction operator preserves the key features of the image by relying on an aggregation-based strategy. To further enhance the robustness of the method, a smoothing procedure is applied to the prolongation operator.

For the sake of simplicity, we employ a gradient descent method as the smoother; however, more sophisticated iterative methods can also be considered. Numerical results confirm an acceleration of convergence, even for aggressive coarsening. Moreover, in addition to accelerating convergence, a slight improvement in reconstruction quality is observed when the method is combined with a discrepancy principle stopping criterion.

Keywords: Image deblurring · Multilevel methods · Segmentation

1 Introduction

Image deblurring is a fundamental task in applied science, consisting of recovering an image from observed data that has been corrupted by measurement error or from insufficient information. Typically, an image deblurring problem is expressed as a linear system where the matrix A, which is the discretization of a convolution operator, acts on an image x, producing a blurred image b by the equation

$$Ax = b, \tag{1}$$

see [10]. The error-free image b is not available in practice due to the presence of measurement errors or due to discretization error, and we have access only to the corrupted signal b^δ such that

$$\|b - b^\delta\| < \delta, \tag{2}$$

© The Author(s), under exclusive license to Springer Nature Switzerland AG 2027
O. Gervasi et al. (Eds.): ICCSA 2026 Workshops, LNCS 16763, pp. 108–123, 2027.
https://doi.org/10.1007/978-3-032-30530-5_7

where $\delta > 0$ is an estimation of the noise level [8]. The goal is to recover an approximation of x from an observed blurred and noisy image b^δ. In order to simulate real-world conditions, we assume a white Gaussian noise of level δ. Thus, our problem can be modeled as the linear system

$$Ax = b^\delta. \tag{3}$$

Due to the presence of noise, it is natural to look for the solution of a least square problem

$$\min_{x \in \mathbb{R}^n} \|Ax - b^\delta\|. \tag{4}$$

Since the gradient of the objective function is $A^T(b^\delta - Ax)$, where A^T is the transpose of A, the gradient descent method, also known as Landweber method [8], can be formulated as the following

$$x_{k+1} = x_k - \alpha_k A^T(Ax_k - b^\delta), \tag{5}$$

where $\alpha_k > 0$ is the step length. In practice, the typical behavior of the error norm of the computed approximation is that it decreases during the initial iterations, when the regularization error dominates, and then starts to increase after a certain iteration, as the noise error begins to amplify the norm of the reconstruction. This behavior of iterative methods applied to discretized inverse ill-posed problem is known as semi-convergence. Therefore, early stopping is crucial for obtaining accurate reconstructions. A classical strategy is to stop the iterative method (5) at the first iteration for which the norm of the residual is close to the noise level δ in (2).

Image segmentation algorithms partition an image's pixels into regions that are similar with respect to certain features. Common features include spatial proximity and grayscale similarity. Image segmentation aims to provide a lower-dimensional representation of the image, in which the identified regions offer a simpler yet effective description of the original image. The application of these algorithms in computer vision and pattern recognition has been widely successful. Various strategies have been proposed to obtain meaningful segmentations and to apply them to real-world problems [1,9].

Multigrid algorithms, originally developed for solving linear systems arising from partial differential equations, have also been applied to ill-posed problems such as image deblurring [4,6,7,12,13]. These methods are based on the definition of grid transfer operators that "transport" information across different levels of the problem in a hierarchical manner. Classical choices for prolongation and restriction operators include downsampling—typically combined with full weighting over pixel neighborhoods—interpolation, and aggregation [14,16]. Since aggregation-based grid transfer operators are often not sufficiently effective on their own, they are commonly combined with a smoothing procedure, leading to smoothing aggregation multigrid methods [3,15].

To the best of our knowledge, the use of segmentation algorithms within a multigrid or multilevel framework for imaging has not yet been explored. Moreover, they have not been used to define the restriction and prolongation operators

required in a multigrid approach. The possibility of defining grid transfer operators based on image segmentation provides a framework for exploring nonstandard properties of multigrid methods in imaging, beyond the image deblurring application considered in this paper. This approach can be interpreted as a data-dependent version of the multigrid framework, since the grid transfer operators are constructed from the observed image. This may lead to coarse representations of the original problem that are more meaningful than those obtained using standard restriction operators, regardless of the images in question.

In this work, we restrict our attention to the study of a cascadic multilevel approach developed in [12,13]. This approach differs from the classical multigrid framework in [4,7] in that the image is first restricted to a coarser level and, once an approximate solution has been computed using an iterative method, it is prolonged to the finer level, where further iterative refinement is performed by means of an iterative solver. Our proposal differs from that in [12,13] in the choice of the grid transfer operators, as we define both restriction and prolongation operators based on a segmentation obtained via a segmentation algorithm [1,9]. The main difficulty in the cascadic approach lies in the definition of suitable stopping criteria for the coarse-level problems. Here, we extend the analysis in [12,13] by proposing a suitable variant of the discrepancy principle.

This paper is organized as follows. Sections 2 and 3 introduce the two main components of our method: cascadic multigrid methods and segmentation algorithms. A detailed analysis of a variant of the discrepancy principle as a stopping criterion at the coarsest level is presented in Sect. 4. Section 5 is devoted to a set of numerical experiments demonstrating the robustness of the proposed two-level method, even in the case of aggressive coarsening.

2 Cascadic Multigrid

In [12], the authors proposed the use of a cascadic multilevel approach to solve image deblurring problems as (3). A multilevel method is characterized by a chain of nested subspaces $W_1 \subseteq W_2 \cdots \subseteq W_l = \mathbb{R}^n$. We will refer to the subspaces W_i as levels and we will say that W_i is coarser respect to W_{i+1} while W_{i+1} is finer respect to W_i. In order to move between the different levels, we need to define the restriction and prolongation operators. In a cascadic multiresolution approach, the restriction operator, usually denoted by R_i, is defined as $R_i : \mathbb{R}^n \to W_i$ while the prolongation operator is defined as $P_i : W_i \to W_{i+1}$.

The cascadic multilevel approach strategy aims to compute an approximate solution for the problem (3) at the coarsest level W_1 by means of an iterative solver. Then the prolongation operator P_1 is applied to this coarse solution to compute an initial guess for the level W_2. Once we are working in W_2, a correction of the initial approximation is computed and the iterative method is stopped, this new corrected solution is mapped to the finer level and corrected again. The procedure is presented in Algorithm 1.

Algorithm 1. Multilevel algorithm from [12]

Input: A, b^δ, δ, l the number of levels, an *IterativeMethod* and a stopping rule.
Output: An approximate solution $\tilde{x}$ in W_l

```
for i = 1, ..., l do
    compute A_i and b_i^δ
end for
x_0 = 0
for i = 1, ..., l do
    x_{i,0} = P_i x_{i-1}
    Δx_{i,k_i} = IterativeMethod(A_i, b_i^δ − A_i x_{i,0})
    correction step: x_i = x_{i,0} + Δx_{i,k_i}
end for
x̃ = x_l
```

The *IterativeMethod* is stopped at iteration k_i at the $i-$it level according to the stopping rule. It is applied to the error equation end hence $\Delta x_{i,k_i}$ is an approximation of the error at the $i-$th level.

We stress that this framework of the cascadic multigrid is independent of the choice of the restriction and prolongation operators. In this work, we explore the possibility of using restriction and prolongation operators defined starting from a segmentation of the observed image. Moreover, we consider only a 2-level cascadic approach. Therefore, we consider only two levels denoted as $W_c \subseteq W_f = R^n$. We will denote with $b_f^\delta, b_c^\delta, A_f$, and A_c, respectively, the observed signals and the operators at the coarse and fine level, respectively. Moreover, since we are dealing with only two levels, we will simply denote the restriction operator by R and the prolongation operator by P.

3 Segmentation and Coarsening

The output of any segmentation algorithm can viewed as a function that, given an input image $I \in \mathbb{R}^n$, provides a collection of elements $\mathcal{L} = \{\ell_1, \ldots, \ell_m\}$ and a function $\mathcal{P} : \mathcal{L} \times \mathbb{R}^n$ s.t.

$$\mathcal{P}(\ell_i, p) = \begin{cases} 1 \text{ if } p \in \ell_i \\ 0 \text{ otherwise,} \end{cases} \tag{6}$$

where $p \in \mathbb{R}^N$ are the pixels of the image I. The function (6) identifies if a pixel belongs to the element ℓ_i or not. For convenience, we denote the cardinality of ℓ_i by $\#\ell_i$ and the cardinality of the segmentation as $\#\mathcal{L} = m$.

We define the coarse level as $W_c = \mathbb{R}^{\#\mathcal{L}}$, which is the space of the elements of the segmentation of the observed image. Once we have a segmentation $\mathcal{L}$, we need to associate a value at each $\ell_i \in \mathcal{L}$. We select for this the mean of the values in the element. This choice resemble the standard multilevel choice of local

averaging on the pixels of the image.

More formally, the restriction operator $R : W_f \rightarrow W_c$ is defined as the average value of each pixel belonging to the same element of the segmentation. It is the product of the matrix $\Pi : \mathbb{R}^n \rightarrow \mathbb{R}^m$, which is the binary matrix that is 1 where $\mathcal{P}$ in Eq. (6) is, and the diagonal matrix Λ with diagonal entries $\Lambda_{i,i} = \text{Diag}(1/\#\ell_i)$.

Namely, we define the restriction operator as

$$R = \Lambda\Pi. \tag{7}$$

Fig. 1 show a visual representation of the application of the restriction operator R to an image.

In order to define a coarse representation A_c of the fine blurring operator $A_f = A$, we use a Galerkin approach such that

$$A_c = \Lambda\Pi A_f \Pi^T, \tag{8}$$

according to the choice $P = \Pi^T$.

The problem with this choice of P is that the prolonged image in W_f will result in a linear piecewise representation of the element of the segmentation. To avoid this problem, we define the prolongation operator as

$$P = G \star \Pi^T, \tag{9}$$

where $\star$ is the convolution operator and G is a Gaussian kernel of standard deviation 1. This has been performed to smooth the approximated solution on the fine grid, reducing the effect of the piecewise constant approximation that will result from the prolongation alone. With this new choice of the prolongation the coarser operator A_c in (8) is no longer associated to the Galerkin approach, which exhibits an increase in ill-conditioning at high frequencies. Anyway, the test performed with the Galerkin approach gives comparable results and hence we prefere to keep the coarser operator as A_c in (8), since it is cheaper to compute and better conditioned with respect to the true Galerkin operator.

Note that the prolongation P in Eq. (9) apply a smoothing step, by the Gaussian kernel, to the aggregation grid transfer operator. Indeed, a higher variance of the Gaussian kernel G can be interpreted a more steps of the smoothing of the aggregation prolongation [3]. Finally, when the segmentation algorithm provides a degenerate grid with a large variation in $\#\ell_i$, then the coarse operator A_c becomes more and more ill-conditioned leading to a decline in performance.

4 Stopping Criterion for Cascadic Multilevel

In order to find the approximate solution at every level, a stopping criterion is needed. This criterion must hold both for the fine and coarse levels. In [12,13]

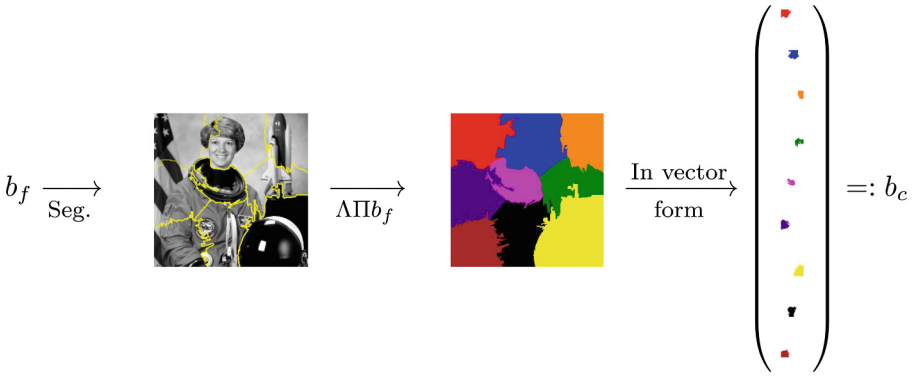

Fig. 1. Visual representation of the action of the restriction operator. Different colors represent different values.

the authors propose to use a variant of the Discrepancy Principle (DP) as a stopping rule at the coarse levels. We briefly recall the DP and the extension presented in the articles. Then, we further extend the stopping criterion to the coarsening based on a segmentation.

Given $v \in \mathbb{R}^n$, we define the weighted least squares norm as

$$\|v\| = \frac{1}{\sqrt{n}}\|v\|_2, \tag{10}$$

and we assume that we know an estimate of norm of the noise $\delta = \|b^\delta - b\|$, where b denotes the blurred but noise-free image. A vector x is said to satisfy the Discrepancy Principle (DP) if $\|Ax - b^\delta\| < \gamma\delta$, for a fixed $\gamma > 1$. Given an iterative method, the stopping rule based on the DP terminates the iterative process at the first step k such that

$$\|Ax_k - b^\delta\| < \gamma\delta. \tag{11}$$

Starting from this stopping criterion, the authors propose to extend it to the cascadic multilevel setting.

In Algorithm 1, the *IterativeMethod* is applied to the linear system $A\Delta x_i = b_i^\delta - A_i x_{i,0}$ and stopped by DP. In order to stop the iteration at the i-th level, let c_i be such that $\|b_i^\delta - b_i\| \leq c_i\delta$, we terminate the iteration of the *IterativeMethod* at level i when

$$\|b_i^\delta - A_i x_{i,0} - A_i \Delta x_{i,k_i}\| \leq c_i\delta, \quad i = 1, \ldots, l. \tag{12}$$

where $c_l = \gamma$ and k_i is the $k-$th iteration at the $i-$th level. In the case where the restriction operator coincides with the weighted average of four adjacent pixels, the authors [12] proved that the relation $c_i = \frac{1}{2}c_{i+1}$ holds.

4.1 Estimation of c_1 in the Segmentation Case

Since we are considering a 2-level method, we need to determine a constant c_1 that must hold at the coarse level. To compute this constant, first consider the coarse residual $e_c = b_c^\delta - b_c$. We define the average variance norm of e_c given a segmentation $\mathcal{L}$ as

$$\|e_c\|_V^2 = \frac{1}{\#\mathcal{L}} \sum_{\ell_i \in \mathcal{L}} \mathrm{Var}(e[\ell_i]), \tag{13}$$

where $e[\ell_i] = \frac{1}{\#\ell_i} \sum_{p \in \ell_i} e^p$ is the mean with respect to the element ℓ_i and e^p is the $p-$th entry of e. Therefore, by the properties of the variance, we have

$$\|e_c\|_V^2 = \frac{1}{\#\mathcal{L}} \sum_{\ell_i \in \mathcal{L}} \frac{1}{\#\ell_i^2} \sum_{p \in \ell_i} \mathrm{Var}(e^p). \tag{14}$$

By observing that $\sum_{\ell_i \in \mathcal{P}} \sum_{p \in \ell_p} \mathrm{Var}(e^p) = \sum_{i=1}^n \mathrm{Var}(e^i)$, we obtain

$$\frac{n}{\#\mathcal{L} \cdot \max(\ell_i)^2} \|e_f\|_V^2 \quad \leq \|e_c\|_V^2 \leq \quad \frac{n}{\#\mathcal{L} \cdot \min(\ell_i)^2} \|e_f\|_V^2. \tag{15}$$

Using the approximation $\|e_f\|_V \approx \delta$, we define

$$c_{max} = \gamma \sqrt{\frac{n}{\#\mathcal{L} \max(\ell_i)^2}}, \quad c_{min} = \gamma \sqrt{\frac{n}{\#\mathcal{L} \min(\ell_i)^2}}, \quad c_{avg} = \frac{c_{min} + c_{max}}{2}. \tag{16}$$

We observe that c_{min} and c_{max} in (16) depend on the segmentation; in particular, they depend only on the minimum and maximum number of pixels present in an element of the segmentation. The choice $c_1 = c_{min}$ is consistent with the stopping criterion (12). In practice, $c_1 = c_{avg}$ usually provides a good choice in the numerical experiments.

Example 1. If we consider the case where the restriction operator is the average of four adjacent pixels in the image, we have that $\#\mathcal{L} = n/4$ and $\min(\#\ell_i) = \max(\#\ell_i) = 4$, thus Eq (15) leads to

$$\frac{1}{4}\|e_f\|_V^2 \leq \|e_c\|_V^2 \leq \frac{1}{4}\|e_f\|_V^2. \tag{17}$$

Thus, the same conclusion obtained in [12] that $c_1 = \frac{1}{2} c_f$ holds.

5 Numerical Experiments

In this section, we present three numerical experiments. For all the numerical experiments, we consider the 2-level method proposed. Firstly, we obtain the initial segmentation computed on the corrupted observed image by means of two well-known segmentation algorithms: SLIC [1] and Felzenszwalb's algorithm [9]. For both algorithms, we use the versions implemented in the scikit-image library [17]. The Landweber method is used as an iterative solver in Algorithm 1. We consider Algorithm 1 where, after the segmentation is obtained, we project the

image on the coarse level, then we obtain a reconstruction at the coarse level by means of Landweber, we prolong it to the fine level, and correct it.

In each test, we consider a test image that is blurred using two different kernels, then additive white Gaussian noise is added to the image. We add the noise ξ such that b^δ is computed as

$$b^\delta = b + \delta\xi \tag{18}$$

and we denote by δ the noise level. The parameter γ for the Discrepancy Principle (11) is set to 1.01 while, for the Landweber steplenght α_k we use a constant choice of $\alpha_k = \frac{1}{\|A\|_2^2}$ at the fine level and $\alpha_k = \frac{1}{\|A_c\|_2^2}$ and at the coarse level. In the last numerical experiment, we use CLGS instead of Landweber as iterative solver.

5.1 First Numerical Experiment: Gaussian Blur and 0.5% of Noise Level

We consider the 256×256 test image in Fig. 2. The true image is corrupted by the convolution with a Gaussian kernel with a standard deviation of 5 and additive white Gaussian noise of level 0.5%. The cropped PSF, i.e., the convolution operator applied to a point, is reported in Fig. 2. The segmentation is obtained by applying the SLIC algorithm directly on the observed corrupted image. The resulting segmentation consists of 53 elements.

In Fig. 3, we report the approximations obtained via the proposed 2-level method and the one obtained with the standard Landweber method. For comparison, we report the value of the PSNR and the SSIM for both images in the caption.

In Fig. 4, the evolution of the PSNR against the number of iterations is shown for both the two-level method and the Landweber method. We observe that the proposed method consistently produces approximations with higher PSNR values. Moreover, the standard Landweber method requires approximately twice as many iterations to achieve comparable PSNR values. The number of iterations performed at the coarse level is 5, which is negligible compared to the number of fine-level iterations.

5.2 Second Numerical Experiment: Box Blur and 2% of Noise Level

As a second test, we consider the 256×256 test image in Fig. 5, the image is corrupted by a box blur and a noise level of 2% is added. The corrupted image and the PSF are reported in Fig. 5. In this test, we consider Felzenszwalb's algorithm for the segmentation. This algorithm gives rise to segmentations that are less regular with respect to the segmentations obtained using the SLIC algorithm, as we can observe in the segmentation presented in Fig. 5.

The resulting segmentation consists of 126 elements. In Fig. 6, the approximated solutions obtained by Landweber and the proposed method are presented.

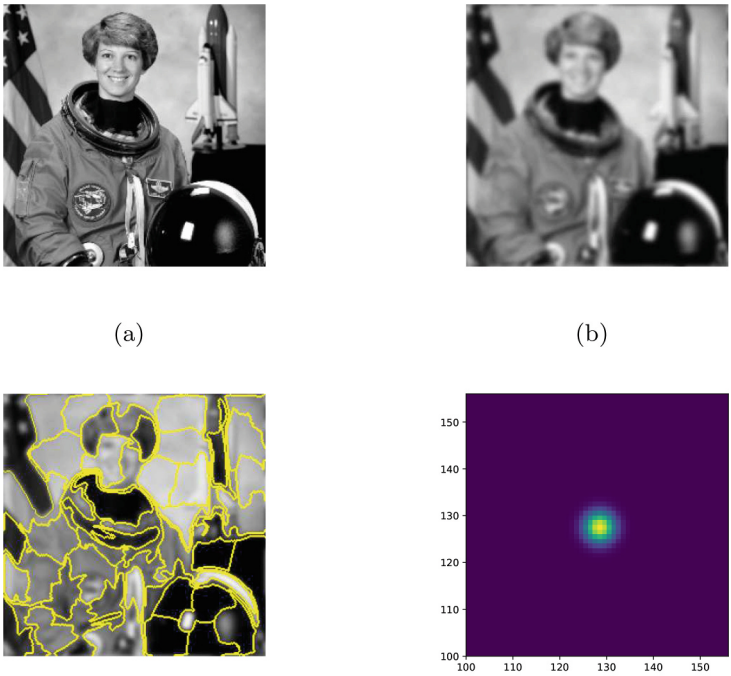

Fig. 2. (a) Original test image, (b) corrupted observed image, (c) segmentation used, (d) PSF used in the test.

Figure 7 shows the evolution of the performance metric against the number of iterations. The iterations performed at the coarse level are 2.

According to the results of the first experiment, we observe that the cascadic 2-level method improves the reconstruction and, in a number of fine iterations that are comparable to standard Landweber, returns an approximation with higher value of PSNR. If we consider the evolution of the iterations, we observe that the 2-level method obtains reconstructions that are with a better PSNR value.

5.3 Third Numerical Experiment: Test with Different Segmentation Sizes

As an additional test, we investigate the effect of the starting segmentation on the evolution of the performance metrics. We compute three initial segmentations using the SLIC algorithm that are of different sizes: 62, 248, and 521. In this test, we are considering a noise level of 1% and a Gaussian blur of standard deviation 3. In Fig. 8 we present the three initial segmentations proposed, the PSF, and the evolution of the PSNR for the 2-level cascadic algorithm as well



(a)



(b)

Fig. 3. (a) Landweber method PSNR: 23.12 SSIM: 0.792, (b) 2-level cascadic PSNR: 23.32 SSIM: 0.795

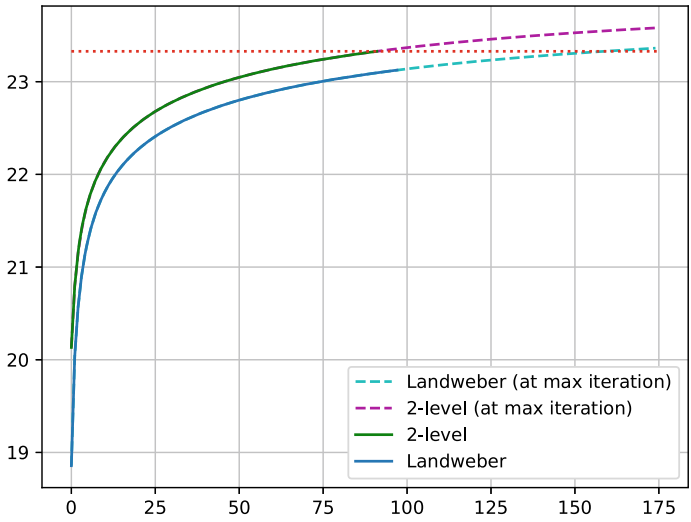

Fig. 4. PSNR value against the iteration number. The red dotted line represents the PSNR value reached for the 2-level method. (Color figure online)

as for standard Landweber. We observe that using a larger number of segmentation elements leads to higher PSNR values. However, the improvement over segmentations with fewer elements is marginal.

5.4 Fourth Numerical Experiment: Test Using CGLS Instead of Landweber

To prove the flexibility of our 2-level approach, we replace the Landweber iteration with the CGLS method [2] in Algorithm 1. We perform the same experiment as in Subsect. 5.1 cf. Fig. 2. As in the previous test, a noise level of 0.5% is added. The final reconstructions obtained with both CGLS and the 2-level

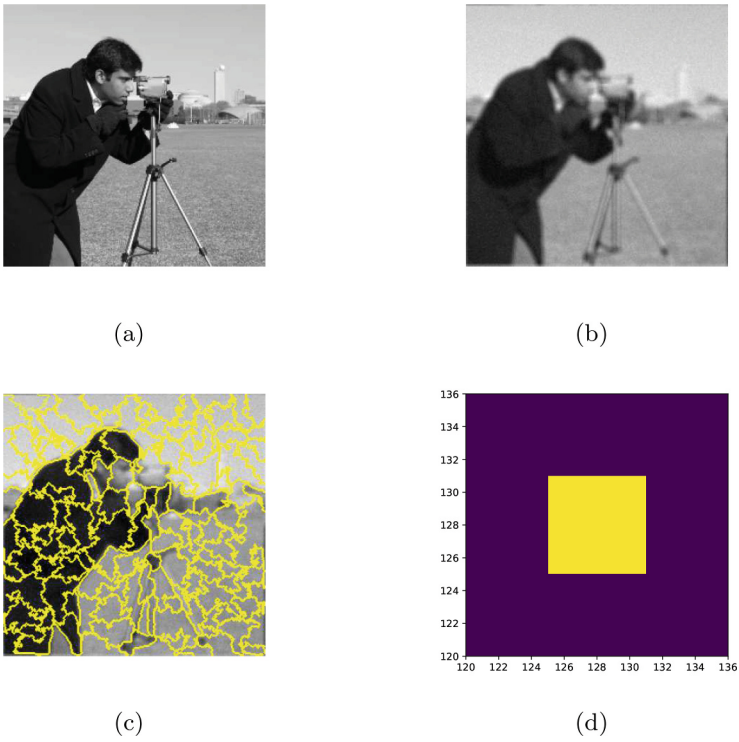

Fig. 5. (a) Original test image, (b) corrupted observed image, (c) segmentation used, (d) PSF used in the test.

method with CGLS as standard iterative solver are reported in Fig. 9. The corresponding performance metrics are reported in the caption. The number of iterations performed at the coarse level is 4.

In Fig. 10, we report the evolution of the performance metrics against the iteration number. As expected, the CGLS method converges faster than the Landweber method. Moreover, in accordance with the previous tests, the proposed 2-level method produces reconstructions with higher PSNR values in fewer iterations with respect to the standard iterative method.



(a) (b)

Fig. 6. (a) Landweber method PSNR: 23.87 SSIM: 0.652, (b) 2-level cascadic PSNR: 24.02 SSIM: 0.657

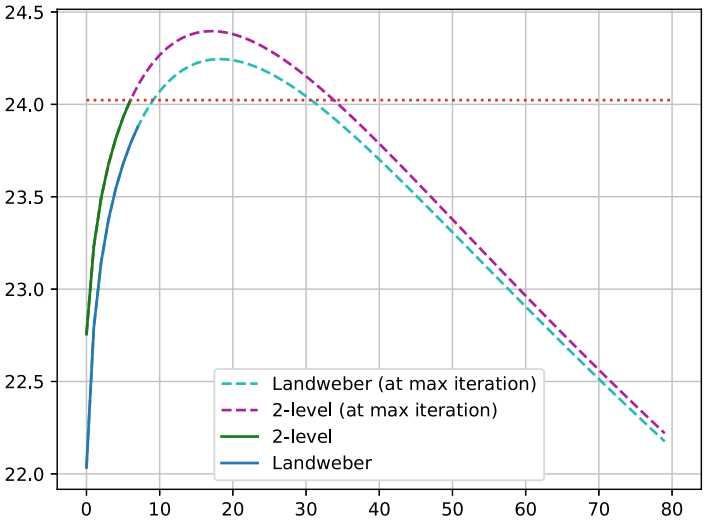

Fig. 7. PSNR value against the iteration number. The red dotted line represents the PSNR value reached for the 2-level method. (Color figure online)



(a)

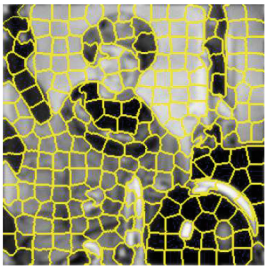

(b)

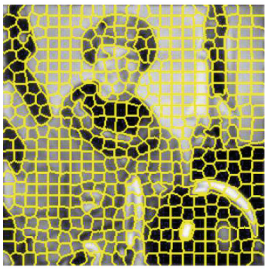

(c)

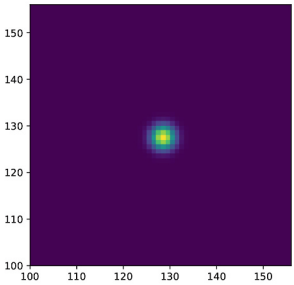

(d)

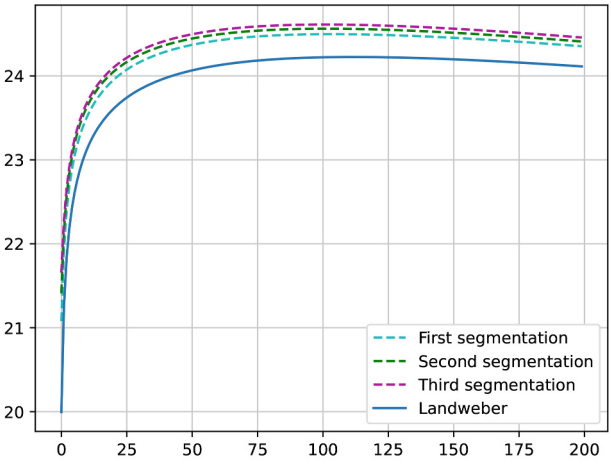

(e)

Fig. 8. (a) First segmentation of 62 elements, (b) second segmentation of 248 elements, (c) third segmentation of 521 elements, (d) evolution of the PSNR for the three segmentations and the standard Landweber against the iteration number.



(a) (b)

Fig. 9. (a) CGLS solution PSNR: 23.18, SSIM: 0.782, (b) 2-level solution PSNR: 23.39, SSIM: 0.788

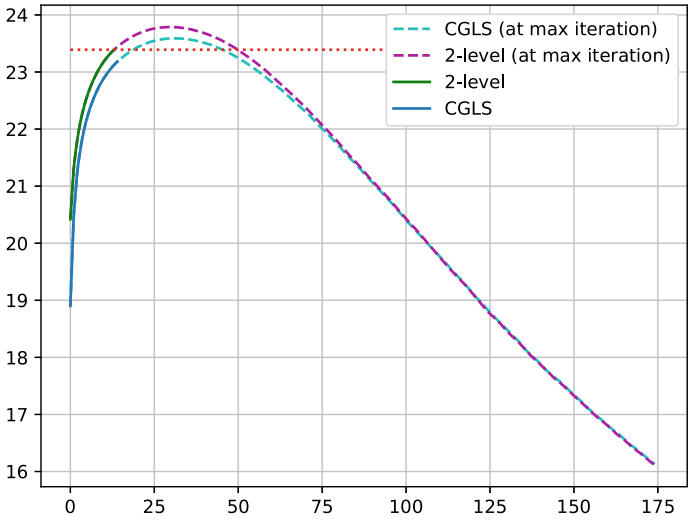

Fig. 10. Evolution of the PSNR against the number of iterations. The red dotted line represents the PSNR value reached for the 2-level method. (Color figure online)

6 Conclusions

In this work, we investigated the possibility of using nonstandard, segmentation-aware grid transfer operators in a cascadic multigrid setting. We then derived a stopping criterion for the coarse level. The numerical experiments with different blurring operators and noise levels confirm the robustness of the proposed two-level method, even under aggressive coarsening projections. The initial computation of the projection operator necessarily introduces computational overhead. This overhead depends on both the time complexity of the initial segmentation and the cost of the projection at the coarse level. The time complexity for the initial segmentation is $O(N)$ for SLIC [1] and $O(N \log N)$ for Felzenszwalb's

algorithm [9]. In addition, the cost of projecting the problem at the coarse level must be taken into account. The use of these operators in a non-cascadic multilevel setting remains to be explored, as does their extension to more than two levels. Moreover, the adoption of other iterative solvers, such as the iterative soft-thresholding algorithm and its accelerated versions [5,11], should be considered. The use of an iterative soft-thresholding algorithm, which aims to promote sparsity with respect to a given basis (e.g., wavelets) at the coarse level, inherently requires the definition of both the projection onto the chosen basis and the optimization problem to be solved at that level.

Acknowledgments. The authors thank Professor Rolf Krause for the valuable discussions that contributed to this work, in particular for his insights into multigrid algorithms. The authors are partially supported by the Italian Ministry of the University and Research, through the PRIN 2022 project "Inverse Problems in the Imaging Sciences (IPIS)" (No. 2022ANC8HL), and GNCS–INdAM.

Disclosure of Interests. The authors have no competing interests.

References

1. Achanta, R., Shaji, A., Smith, K., Lucchi, A., Fua, P., Süsstrunk, S.: SLIC superpixels compared to state-of-the-art superpixel methods. IEEE Trans. Pattern Anal. Mach. Intell. **34**(11), 2274–2282 (2012)
2. Björck, Å.: Numerical Methods for Least Squares Problems, 2nd edn. Society for Industrial and Applied Mathematics, Philadelphia, PA (2024)
3. Bolten, M., Donatelli, M., Huckle, T., et al.: Analysis of smoothed aggregation multigrid methods based on Toeplitz matrices. Electron. Trans. Numer. Anal. **44**, 25–52 (2015)
4. Buccini, A., Donatelli, M.: A multigrid frame based method for image deblurring. Electron. Trans. Numer. Anal. **53**, 283–312 (2020)
5. Daubechies, I., Defrise, M., De Mol, C.: An iterative thresholding algorithm for linear inverse problems with a sparsity constraint. Commun. Pure Appl. Math. A J. Issued by the Courant Institute Math. Sci. **57**(11), 1413–1457 (2004)
6. Donatelli, M.: A multigrid for image deblurring with Tikhonov regularization. Numer. Linear Algebra Appl. **12**(8), 715–729 (2005)
7. Donatelli, M., Serra-Capizzano, S.: On the regularizing power of multigrid-type algorithms. SIAM J. Sci. Comput. **27**(6), 2053–2076 (2006)
8. Engl, H.W., Hanke, M., Neubauer, A.: Regularization of inverse problems, vol. 375. Springer Science & Business Media (1996)
9. Felzenszwalb, P.F., Huttenlocher, D.P.: Efficient graph-based image segmentation. Int. J. Comput. Vis. **59**(2), 167–181 (2004)
10. Hansen, P.C., Nagy, J.G., O'Leary, D.P.: Deblurring images: matrices, spectra, and filtering. SIAM (2006)
11. Huang, J., Donatelli, M., Chan, R.H., et al.: Nonstationary iterated thresholding algorithms for image deblurring. Inverse Probl. Imaging **7**(3), 717–736 (2013)
12. Morigi, S., Reichel, L., Sgallari, F.: Noise-reducing cascadic multilevel methods for linear discrete ill-posed problems. Numer. Algorithms **53**(1), 1–22 (2010)
13. Morigi, S., Reichel, L., Sgallari, F., Shyshkov, A.: Cascadic multiresolution methods for image deblurring. SIAM J. Imaging Sci. **1**(1), 51–74 (2008)

14. Notay, Y.: An aggregation-based algebraic multigrid method. Electron. Trans. Numer. Anal. **37**(6), 123–146 (2010)
15. Vaněk, P., Brezina, M., Mandel, J.: Convergence of algebraic multigrid based on smoothed aggregation. Numer. Math. **88**(3), 559–579 (2001)
16. Vaněk, P., Mandel, J., Brezina, M.: Algebraic multigrid by smoothed aggregation for second and fourth order elliptic problems. Computing **56**(3), 179–196 (1996)
17. van der Walt, S., et al.: scikit-image contributors: scikit-image: image processing in Python. PeerJ **2**, e453 (2014)